Finite element analysis of individual taenioglossan radular teeth (Mollusca)

Wencke Krings[1]*, Jordi Marcé-Nogué[234], Hasan Karabacak[1], Matthias Glaubrecht[1], Stanislav N. Gorb[5]

[1] Center of Natural History (CeNak), Universität Hamburg, Martin-Luther-King-Platz 3, 20146 Hamburg, Germany

[2] Department of Pathology and Anatomical Sciences, Jacobs School of Medicine and Biomedical Sciences, University of Buffalo, State University of New York, NY, USA

[3] Department of Mechanical Engineering, Universitat Rovira i Virgili, Tarragona, Spain

[4] Institut Català de Paleontologia Miquel Crusafont, Universitat Autònoma de Barcelona, Barcelona, Spain

[5] Functional Morphology and Biomechanics, Zoological Institute of the Christian-Albrechts-Universität zu Kiel, Am Botanischen Garten 9, 24118 Kiel, Germany

*corresponding author: wencke.krings@uni-hamburg.de; +49 40 428388126, Center of Natural History (CeNak), Universität Hamburg, Martin-Luther-King-Platz 3, 20146 Hamburg, Germany

Abstract

Molluscs are a highly successful group of invertebrates characterised by a specialised feeding organ called the radula. The diversity of this structure is associated with distinct feeding strategies and ecological niches. However, the precise function of the radula (each tooth type and their arrangement) remains poorly understood. Here for the first time, we use a quantitative approach, Finite-Element-Analysis (FEA), to test hypotheses regarding the function of particular taenioglossan tooth types. Taenioglossan radulae are of special interest, because they are comprised of multiple teeth that are regionally distinct in their morphology. For this study we choose the freshwater gastropod species *Spekia zonata*, endemic to Lake Tanganyika, inhabiting and feeding on algae attached to rocks. As a member of the African paludomid species flock, the enigmatic origin and evolutionary relationships of this species has received much attention. Its chitinous radula comprises several tooth types with distinctly different shapes. We characterise the tooth's position, material properties and attachment to the radular membrane and use this data to evaluate 18 possible FEA scenarios differing in the above parameters. Our estimations of stress and strain indicate different functional loads for different teeth. We posit that the central and lateral teeth are best suitable for scratching substrate loosening ingesta, whereas the marginals are best suited for gathering food particles. Our successful approach and workflow are readily applicable to other mollusc species.

Keywords

Functional morphology, FEA, radula, mechanical properties, Gastropoda

1. Introduction

1.1 Success of mollusks

Mollusca is the second most taxonomically diverse animal group: estimates comprise 70,000–76,000 [1], up to 130,000 [2], or 200,000 [3–5] extant species. Within Mollusca, even though there are many problems with recording the malacofauna and species numbers [6], Gastropoda is the most diverse constituent clade with 80,000 [7] described recent species. The Molluscan diversity, dating back to more than 550 million years [8–9], is enabled by the colonialization of nearly all aquatic and terrestrial ecosystems leading to the establishment of different ecological niches [10]. This evolutionary success became possible due to the immense diversity in their body plans and shells, their complex nervous systems [10–12], and partially due to a key innovation for mechanical food processing termed radula resembling an important autapomorphy, a distinct feature that is unique to Mollusca.

1.2 Previous work on radular basic structure

The gastropods' feeding organ, the buccal mass, does not only include the radula, but also odontophoral cartilages, muscles, and in some taxa the jaw. The cartilages are covered by the chitinous radular membrane [13], embedding rows of sometimes mineralized teeth [Krings et al., accepted for publication in Malacologica]. During foraging the membrane is pulled over the odontophoral cartilage by radular muscles, leading to the interaction of teeth with the ingesta and substrate (Fig. 1b). This action can lead to wear and potentially structural failure, but the radula is continuously formed at its posterior end(building zone, radular sack) and in the course of an individual ontogeny become mature before entering the working zone whereas at its anterior end the teeth of the outermost row break loose (wearing zone) [14–22].

1.3 Previous work on radular diversity and material properties

The notification that radulae differ in the amounts and arrangements of teeth led to the definition of about 5–7 basic radular types [23–25] which do not consistently reflect phylogeny due to convergences [26]. The tooth morphologies can be distinct between the radular 'morphotypes' but also within each radula (e.g. taenioglossan radula with three morphologically distinct tooth types per row: one central tooth, two lateral teeth and two marginal teeth (Figs. 1c-h, 2). Additionally, radulae can be taxon-specific regarding their tooth morphologies, even in closely related species (e.g. the Paludomid species flock in Lake Tanganyika, [27]). This recognition led to Troschel [28] introducing this character complex as most important for mollusc systematics, resulting in Thiele [29] revising the Mollusca based on these new observations. Nowadays radular tooth morphologies are still understood as of systematic value, but not at every level due to ecological adaptations. Additionally, material properties seem to be diverse in radular teeth. Especially the studies on Patellogastropoda and Polyplacophora show that elements, e.g. Fe, can be incorporated in the chitin matrix probably leading to a greater wear resistance [e.g. 30–43]. The different proportions of the found chemical constituents are thought to cause the measured mechanical properties of the previously studied Patellogastropoda and Polyplacophora species [e.g. 40, 42, 44–46].

1.4 Previous work on radular function

The morphology, position and chemical composition are widely considered adaptive to ingesta or substrate – linking the organism as interface with its environment. Hypotheses relating the radula with the evolution of feeding strategies and trophic specialization have been put forward [47, 48]. There are famous examples of gastropod species that are active predators [e.g. *Conus*]; but many gastropod feed on endolithic and epilithic algae that are rasped from the substrate [e.g. Sacoglossa, 49–53]. The notification that gastropods selectively forage on algae in response to the position, mode of attachment, toughness and cells size have led to the notion of competition avoidance [25, 54, 55]. Additionally, the substrate that the food lies on or is attached to could influence the mechanical composition of radular teeth [see also Krings et al., under review in BMC Evolutionary Biology]. The assumptions that feeding from rocky substrate is enabled by teeth with an upright standing, hard cusp [37, 56] and that those morphs evolved convergently several times [e.g. 57] have been postulated. However, the evolutionary responses to substrate and food is still poorly understood, because current models are descriptive reports on 'differences' in tooth shape and hypotheses derived from these observations [58, 59] but not functional or ecological analyses.

1.5 FEA as potential method

To understand the function of morphological structures, biomechanical models and quantifiable characters are necessary. Previous research [60] has highlighted the difficulties of producing models for understanding the functionality of radular teeth, especially since many factors control the morphology (categories of factors as defined by Hickman [60]: phylogenetic, programmatic, constructional, ecological, maturational, degenerative) and further work emphasized the need to understand the radular function [61–64]. Padilla [65] gave a comprehensive summary on the past studies and suggested to apply approaches with high research potential for the future contributing to a deeper understanding of the ecology and evolution through the light of the functional morphology of radular teeth. While experimenting with grazing molluscs, she already developed biomechanical techniques to measure forces that are required to remove algae [66, 67] which was modified by Krings et al. [68] measuring the in vivo forces exerted by the radula. In this context, especially Padilla's [65] the insistence and emphasis on establishing further 'methods for testing and demonstrating function', the necessity to 'integration of structure and function' and to include the 3-dimensional morphology are highly important. She recommended including the shape, the ingesta-tooth interface, the material properties and the teeth's interaction into future considerations on radular evolution.

Finite-element-analysis (FEA), a software-based virtual method dividing a complex shape into smaller simpler shapes, allows to model and test 3-dimensional bodies with defined material properties under the action of outer forces with detailed visualization of deformation and distribution of stresses and strain within the structure. In this context, FEA had been employed in studies of various biological structures including qualitative (stress/strain distribution plots) and quantitative approaches (examining stress/strain at homologous points and comparing the strength of the whole models by computing means). Both, data at homogenous points [69–76] as well as averages are considered valuable in functional-morphological, ecomorphological, and macroevolutionary analyses [77–85] involving standard statistical methods [86–88]. FEA was also applied in studying food processing structures as beaks of Darwin's finches providing engineering evidence for trophic specialization [89] and is a useful approach to provide a comparative perspective on radular teeth mechanics. In Malacological objects FEA had already been used for understanding the functionality of *Patella*, Polyplacophora [37] and *Euhadra* [90] radular teeth. Van der Wal et al. [37] designed a FEA study including considerations on the material gradients and mechanical properties of teeth. However, their study lacks the exact 3D morphology, which at that time could not be included in FEA due to lacking computing capacity. Fortunately, we are capable of this today due to the progress in data processing technology. Additionally, in more recent FEA studies on radular teeth [90] material properties, especially gradients, are lacking. However, since they are of high functional importance [e.g. 91–98] they should be included in FEA [see also 99].

To lay a keystone for further studies that appeal the overflowing diversity of radular teeth and to connect radular diversity with functionality and hence possible adaptations to the ingesta, we propose here the first biomechanical radular tooth model that includes the exact 3D morphology, the position, the embedment and the mechanical properties (material gradients) of different tooth types. We conducted overall 18 different FEA scenarios with the taenioglossan radula of the gastropod *Spekia zonata* [96] (Fig. 1a). This species belongs to the African Paludomidae foraging algae attached to rocky, solid substrates in Lake Tanganyika and was chosen as model because a) its radula, even though taenioglossan radulae usually have morphologically distinct centrals, laterals and marginals, shows very distinct and hence unusual tooth types (Fig. 1c-h) and b) as representative of a flock this species is interesting in the search for drivers in a potential adaptive radiation, especially since the origin and evolution of these Paludomid gastropods have been discussions for decades [e.g. 27, 101–109]. They represent with about 50–70 species a very spectacular species flock among the molluscs, because even though they are closely related, they show an extraordinary interspecific diversity not only in their shell but also their taenioglossan radular tooth morphology [e.g. 27, 103, 110–112]. In the future we hope to address this paludomid tooth diversity by analysing the functionality of more paludomid radular teeth by FEA to discuss the evolution and potential trophic specialization as it has already been done for Darwin's finches [89]. Here we combined the exact 3D morphology with the material properties in connection with the position of the tooth and its embedment in the membrane and conducted 18 FEA scenarios. By altering conditions in the model, we were able to consider the role of a) the tooth morphology, b) the tooth's position on the radular membrane, c) the mode of embedment in the radular membrane, d) the material gradients of the tooth types (Tab. 1). Comparing the results of the stress and strain in the tooth structures between the scenarios allowed us to put forward hypothesises about the functionality of the taenioglossan radular tooth types and the influence of the different conditions on the mechanical behaviour of teeth and their functional constrains. Additionally we would like to highlight the importance of mechanical properties in biological structures. We hope this basic research contributes to the overall topics of functional gradients or to the design of artificial soft graspers as it has been addressed in [113].

2. Materials and Methods

2.1 Specimens

Adult specimens of *Spekia zonata* are inventoried at the Museum für Naturkunde Berlin (ZMB) or the Zoological Museum Hamburg (ZMH) and stored in ethanol. They were collected from stones at the shores of Lake Tanganyika in Burundi (ZMB 220.144) by F. Riedel and at Kalambo Falls Lodge (Zambia) in 2017 (ZMH 150008/999) by Heinz Büscher.

2.2 Morphological analysis and visualization

To obtain a model suitable for FEA the teeth were formed manually. Radular teeth of *S. zonata* are rather small with ~ 130–200 µm length and are of low contrast and thus could not be visualized applying µ-CT technique (employing standard desktop µ-CTs, e.g. the SkyScan 1172 HR micro-CT [Bruker microCT, Kontich, Belgium]), as it has been applied in previous studies on gastropod anatomy [e.g. 114, 115] or radular tooth morphology [43, 44]. To create a 3D model of the distinct taenioglossan radular teeth, radulae of two specimens (ZMB 220.144-1, ZMH 150008/999-4) were extracted, digested with proteinase K following the protocol of [116], cleaned with an ultrasonic bath and mounted on a scanning electron microscopy (SEM) aluminium sample holder. We only dissected two gastropods, because previous research on Paludomidae showed [e.g. 27] that tooth morphologies are rather constant within the same species. To obtain images from all sides of an individual tooth the radula was manually destroyed, teeth were extracted, twisted and mounted (Fig. 1f, h). Then teeth were coated with carbon and visualized employing the SEM Zeiss LEO 1525 (One Zeiss Drive, Thornwood, NY). Using the 3D software Maya 2019 (Autodesk, Inc., San Rafael, USA), the teeth were then formed by hand (Fig. 2) always comparing the model with the SEM images taken from different sides. In the same manner the position and embedment of the teeth within the membrane were reconstructed (Fig. 3a). The one side of the generated model was then cut and mirrored to generate symmetry. Surface irregularities from model generation were repaired using Geomagic Wrap 2017 (3D Systems, Inc., Moerfelden-Walldorf, Germany) and models were converted to CAD file format necessary for using ANSYS FEA Package.

2.3 Material properties

Material properties (Young's modulus) were taken from [56] (Fig. 3b). In that study, radulae from specimens collected in 1995, 2000, and 2018 and subsequently stored in ethanol were embedded in epoxy, polished and hardness and elasticity was measured by nanoindentation. A diamond tip was pressed onto the material under a known load resulting in quantitative variables in the unit of measurement GPa (harder material has a higher GPa). The materials deformation and reformation allowed us to infer the elasticity of the material [see also 117]. Three indentations were made of each marginal tooth (MT), on the basis, stylus and cusp (Fig. 2), and two indentations where made on the lateral tooth (LT) and central tooth (CT), on the stylus and cusp, since those are shorter. The stiffest material (N = 110 fully mineralized teeth) was found in the CT cusps, followed by the LT cups (N = 112 fully mineralized teeth) and finally MT cusps (N = 60 fully mineralized teeth). The mean value of the measured Young's modulus (CT cups: 8.09 ± 0.65 GPa; CT stylus: 6.67 ±0.54 GPa; LT cups: 5.78 ± 0.42 GPa; LT stylus: 4.95 ± 0.49 GPa; MT cusps: 4.60 ± 0.47 GPa; MT stylus: 3.29 ± 0.50 GPa; MT basis: 2.43 ± 0.30 GPa) was assigned to different tooth areas (Fig. 3b) computing the *heterogeneous models*. It was assigned to the points of the models where it was analysed and by employing the thermal diffusion method values were smoothly diffused through the teeth [118].

For the *homogeneous models*, we applied a unique Young's modulus to the whole tooth and the membrane. For the soft embedment we used a E=0.0225 GPa, for the medium-hard embedment we used a E=0.225 GPa, and for the hard embedment we used E=2.25 GPa. This last value corresponds to the softest measured area in the teeth (Young's modulus of the outer marginal tooth basis). Due to the low thickness of the membrane and due to the rapid mechanical changes while drying, we were not able to measure the hardness and elasticity of the membrane by nanoindentation. Therefore, we altered the mechanical properties of this structure in our model. E=2.25 GPa is the hardest and stiffest embedding condition, because preliminary unpublished results suggested that applying of a higher Young's modulus results in a plateau in stress and strain.

2.4 Area of embedment in the radular membrane

Information about the connection between underlying radular membrane and the tooth itself was taken from [Krings et al., accepted for publication in Malacologica]: the membrane and the tooth itself is composed of chitinous bundles [119] consisting of almost parallel fibres running continuously from the membrane into the tooth cusps, connecting the tooth with the membrane directly. The attachment area (the area connecting tooth with membrane) was identified in [Krings et al., accepted for publication in Malacologica] by mounting the radula upside down on a stub and visualizing the attachment by scanning electron microscopy (SEM). This area was transferred into the 3D model (blue area in Fig. 3a) and we applied a lateral elastic stiffness creating a partial restraint of the movement. We adopted the following values for the elastic foundation stiffness: K_{Hard}=75000 N/mm^3, $K_{Medium\text{-}Hard}$=7500 N/mm^3 and K_{Soft}=750 N/mm^3. These values are obtained assuming a thickness of the membrane of d=0.03 mm, when dividing the Young's modulus for the hard, medium-hard and soft cases (E/d).

2.5 Force applied

A force of 1 N was applied to the cusps of different teeth (red areas in Fig. 3c-f, h-j) along the anterior-posterior axis in the anterior direction (Fig. 3e-g) or along the anterior-medial axis (Fig. 3h-j; see also [37]). For the MT we have chosen to apply the force along the anterior-medial axis (Fig. 3h-j) since stress and strain values are smaller (Fig. 3j) in comparison to applying the force in the anterior-posterior axis (Fig. 3e-g). Since the objective of this work was comparing the different scenarios under the action of the same loading conditions, we were not interested in the applying real values of force, but rather to provide a comparison between models under some arbitrary force.

2.6 FEA model

A structural static analysis was performed employing the finite element package ANSYS 17.1 (Ansys, Canonsburg, USA) in a Dell Precision Workstation T7820 with 64 GB RAM. To evaluate the biomechanical behaviour of the radula when feeding 18 different scenarios were designed depending on the tooth type analysed (marginal, central, and lateral tooth), the stiffness of the embedment (soft, medium-hard, and hard) and the distribution of the material properties (homogeneous or heterogeneous/gradient). See Tab. 1 for the list of all the cases. The different feedings scenarios were meshed using the ANSYS mesh module with an adaptive mesh of hexahedral elements [120] resulting in about 100,000 elements per model.

2.7 Average values and quasi-ideal mesh

In this work we computed the average values of von Mises stress and strain. For non-uniform meshes comprising elements of different sizes, we need to consider this non-uniformity in computing these average values. Therefore, we used the mesh-weighted arithmetic mean (MWAM) and the mesh-weighted median (MWM) as proposed by [121]. Alternatively, we computed the von Mises stress and strain in 11 homologous points for all the cases (Fig. 8). Statistical analyses resulting in medians and standard deviations depicted as boxplots were performed with JMP® Pro, Version 13 (SAS Institute Inc., Cary, NC, 1989–2007).

Tab. 1: Summary of the 18 conducted scenarios with the different conditions of the model: embedment hard, medium-hard, soft (including the Young's modulus E of the membrane and the specific weight K); material properties of the teeth either homogenous (including the Young's modulus E of the teeth) or heterogeneous (with the measured material gradients).

Tooth type	Scenario number	Embedding membrane	E membrane (GPa)	K membrane (N/mm3)	Material properties of teeth	E teeth (GPa)
central tooth	1	hard	2.2500	75000	homogeneous	2.2500
	2		2.2500	75000	heterogeneous	gradient
	3	medium-hard	0.2250	7500	homogeneous	0.2250
	4		0.2250	7500	heterogeneous	gradient
	5	soft	0.0225	750	homogeneous	0.0225
	6		0.0225	750	heterogeneous	gradient
lateral tooth	7	hard	2.2500	75000	homogeneous	2.2500
	8		2.2500	75000	heterogeneous	gradient
	9	medium-hard	0.2250	7500	homogeneous	0.2250
	10		0.2250	7500	heterogeneous	gradient
	11	soft	0.0225	750	homogeneous	0.0225
	12		0.0225	750	heterogeneous	gradient
outer marginal tooth	13	hard	2.2500	75000	homogeneous	2.2500
	14		2.2500	75000	heterogeneous	gradient
	15	medium-hard	0.2250	7500	homogeneous	0.2250
	16		0.2250	7500	heterogeneous	gradient
	17	soft	0.0225	750	homogeneous	0.0225
	18		0.0225	750	heterogeneous	gradient

3. Results

Von Mises stress and von Mises strain, their distribution and mean values, were obtained for each scenario. Von Mises stress is an equivalent stress that summarize the nine stress values of the stress tensor in one unique equivalent value, so it makes the comparison between models easier. Despite von Mises stress is a criterion used to analyse stress distribution in the FEA model, similar equations can be used in strain, so we can compute also a unique and equivalent value of strain for each model. Figs. 4 and 5 display the distribution of von Mises stress and strain in each scenario and Figs. 6 and 7 depict the Mesh-Weighted Arithmetic Mean (MWAM) and Mesh-Weighted Median (MWM).

3.1 Von Mises stresses

3.1.1 Effect of model conditions on stress distribution in different tooth types

In all scenarios (for values see Tab. 2) the marginal tooth (MT) always exhibits higher stress values, whereas the central (CT) and lateral teeth (LT) show lower stress values. In each tooth type the highest stress values were obtained for models with material gradients. The models with gradients showed highest stress values for soft, followed by medium-hard and hard embedding. The highest stress values were obtained for the MT with soft embedding and material gradient, followed by MT with a medium-hard embedding and material gradient, and finally MT with hard embedding and material gradient. Both LT and CT showed also the highest stress for soft, whereas medium-hard and hard embedding showed lower stress values. Every tooth type modelled with homogenous material showed a) lower stress values, and b) the same stress values for all embedding modes (Tab. 2).

3.1.2 Homologous points

Von Mises stress in the defined points (Fig. 8; Supplements Tab. 1) on the marginal tooth was always higher at the tooth basis (12.13–15.19 MPa) than at the stylus (0.29–7.13 MPa) or at the cusp (0.51 MPa). As for the MWAM and MWM, the highest forces at the basis were found in the models with gradients (12.13–15.19 MPa) for all types of embedment. For the other defined points in the MT, stress values are slightly different at different model conditions. In the lateral and central teeth, the highest stress values were calculated for scenarios with material gradients and soft embedment, but the range of force values for all points was much smaller (0.04–0.64 MPa). As for the MWAM and MWM, each point of the models calculated without material gradients always showed lower stress and these values were independent from the embedding mode (MT: P1: 12.13–12.16 MPa; P2: 7.14 MPa; P3: 1.22 MPa; P4: 0.29 MPa; P5: 0.51 MPa; LT: P1: 0.03 MPa; P2: 0.34 MPa; P3: 0.44 MPa; CT: P1: 0.17 MPa; P2: 0.05 MPa; P3: 0.14 MPa).

3.2 Von Mises strain

3.2.1 Effect of model conditions on strain distribution in different tooth types

The marginal tooth exhibits the highest von Mises strain values in comparison to the lateral and central one (Tab. 2; Figs. 4–7). However, the values for different model conditions are opposite in comparison with the von Mises stress: the highest strain was obtained for models without material gradients. The models with gradients show, as for the stress, the highest strain values for the soft embedding: both medium-hard and hard embedding models had lower strain values. The highest stress values were calculated for the marginal tooth with soft embedding and material gradients, followed by the MT with a medium-hard embedding with material gradients and the MT with hard embedding with material gradients. Both lateral and central teeth also showed highest stress for the soft, then medium-hard and finally hard embedding (Tab. 2).

3.2.2 Homologous points

Von Mises strain in the defined points (Fig. 8; Supplements Tab. 1) of the marginal tooth basis was always higher (0.0050–0.5389 MPa) than that in the stylus (0.0001–0.3171 MPa) or in the cusp (0.0001–0.0225 MPa). As for the MWAM and MWM, in all points of the MT the highest strain was found for the model scenarios without gradients (0.0001–0.5389 MPa), with soft, then medium-hard, and finally hard embedment. The same holds true for both central and lateral teeth.

Tab. 2: Values of the stress and strain, in Mpa, for the different FEA scenarios.

Tooth type	Scenario	Embedding membrane	Material properties of teeth	Stress MWAM, MPa	Stress MWM, MPa	Strain MWAM, MPa	Strain MWM, MPa
central tooth	1	hard	homogeneous	0.1888929	0.164465000	86.2	75.1
	2		heterogeneous	0.2086405	0.181253171	28.4	24.5
	3	medium-hard	homogeneous	0.1896065	0.166365587	853.3	749.3
	4		heterogeneous	0.2384223	0.205177677	32.7	27.6
	5	soft	homogeneous	0.1895905	0.166362911	8532.4	7493.7
	6		heterogeneous	0.2446671	0.209700000	33.5	28.1
lateral tooth	7	hard	homogeneous	0.2065989	0.161000000	93.8	73.0
	8		heterogeneous	0.2189697	0.174349367	42.6	34.4
	9	medium-hard	homogeneous	0.2074396	0.162210000	931.1	727.2
	10		heterogeneous	0.2686988	0.229189415	52.2	44.6
	11	soft	homogeneous	0.2065989	0.161000000	9382.4	7295.7
	12		heterogeneous	0.2898695	0.245265000	57.0	47.9
outer marginal tooth	13	hard	homogeneous	1.5554244	0.420405942	736.5	194.2
	14		heterogeneous	1.5607737	0.423819854	595.7	102.5
	15	medium-hard	homogeneous	1.5554244	0.420405942	7364.6	1942.3
	16		heterogeneous	1.7632298	0.424554246	699.7	102.5
	17	soft	homogeneous	1.5554244	0.420405942	73645.5	19422.6
	18		heterogeneous	1.9434961	0.424714985	790.9	102.5

4. Discussion

As already proposed by Padilla [65] biomechanical modelling approaches that include the 3-dimensional shape of the tooth, the interaction between the teeth, the material composition, and the interface between tooth and ingesta are crucially important to access the functional significance of morphological structures. Here we provide the first FEA model of taenioglossan radular teeth including these properties. The visual representation of the stress distribution for the FEA models is valuable for comparisons and hypotheses on the biomechanical behaviour.

4.1 Tooth morphology and the position on the radular membrane

The results of the FEA models for the distinct radular tooth types (Figs. 4–7) can be explained by their morphologies: short, broad morphologies will not deform as much as taller, thinner ones. The marginal tooth always experiences higher stress and strain than the central and lateral tooth since the latter ones are rather short and broad (CT width mean value: ~ 170 µm, LT width mean value: ~ 130 µm) important for transferring force effectively to the substrate [see also 52, 56, 65]. CTs and LTs display additionally a thick cutting edge at the interface between the tooth and ingesta. Jensen [52] highlighted different effects of the tooth shape on the ingesta and Padilla [65] pointed out the importance of this contact area since its size determines local pressure (the amount of force per unit area) applied to ingesta. Pointy teeth exhibit a stronger pressure on their tooth cusps which makes them more effective at piercing and tearing whereas blunt teeth, as the CT and LT of *S. zonata*, are presumably more effective for loosening material from substrate surfaces (in this specific case from solid surfaces, see also [52, 56, 65–68]). In *S. zonata* thick rounded bulges are present at the basis of the LT and the CT. The bulges contribute to the reinforcement of the tooth structure and hence support the force transmission to the radular membrane. The MT in contrast consists of rather slender and thin stylus (MT length mean value: ~ 209 µm) with small bulges at the edges reinforcing the structure before terminating in a cusp containing small denticles. In contrast to the hypothesis stating that long teeth are more effective in removing algae tissue [122] these long MT are more affected in our model by stress and strain due to their thinness. In turn this results in higher deformation when in contact with the substrate, but also in an enlarged risk of breaking. This hypothesize on function had already been put foreward in [56, 65, 123] and is now supported by the results of this paper. It is important to note that the modelled highest values of stress and strain were always observed in the thinnest parts of teeth: in the MT at the stylus and denticles, in the LT at the denticles and basis, in the CT at the cutting edge and basis (Figs. 4–5).

Reconstructing the 3D-model gave us insight into the precise position of the teeth to each other. Their arrangement on the radular membrane results in the interaction and interlocking between them. This effect in turn aids in the force transmission from the single tooth to the neighbouring teeth as had been previously postulated by [60] and [65]. The CTs from adjacent rows support each other by the interaction of their bulky bases with the rounded bulges of their styli. The rounded and broad bases of the LT fit perfectly together; hence adjacent tooth rows can stabilize each other while interacting with the substrate surface. The MTs support each other as well: the two marginal teeth – the inner and the outer – can interlock tightly. Here the outer, larger MT embraces the inner, smaller MT; they can hence function as one single unit [62]. The performance of single teeth is of high interest as well [37, 90], but to link morphology and function it is utterly necessary to consider the radula with all its teeth as a complex unit with mechanically interacting, non-independent structures [56, 62, 63, 65].

4.2 Material gradients

Our experiments on models with material gradients (heterogeneous tooth material properties obtained experimentally) resulted in higher values of stress in the teeth (Figs. 5–7) with both central and lateral teeth being less effected than the marginal ones. However, the incorporation of the Young's modulus into our models has stronger effect on the values of the strain than on the values of stress: the strain was much higher in homogenous teeth than in heterogeneous ones showing that homogenous teeth deform more. Van der Wal et al. [37] highlighted the importance of material gradients in radular teeth. They found for *Patella* and representatives of Polyplacophora that the 'leading part' of the tooth (the area of interaction between the tooth and substrate) is harder and stiffer than the 'trailing part'. It seems to be important for its functionality, because hard materials with softer underlying layers might be less prone to abrasion [44, 94, 124 and 125 on snake skin]. Teeth of *S. zonata* are morphologically distinct from the teeth of *Patella* and Polyplacophora, but we also revealed material gradient in the species studied: the cutting edge of the tooth cusps is the hardest and stiffest area, teeth become softer and more flexible over the stylus to the basis [see also 56, 123]. The harder and stiffer material properties in the cusps, especially in the LTs and CTs, are needed for transferring force to the ingesta (in the case of *S. zonata*, teeth acting on algae attached to a rocky surface). This interaction could either lead to natural wear at the cusps documented for gastropods and Polyplacophora [18, 20, 21, 39, 126, 127], but might also result in a risk of fracture when teeth are exposed to higher stresses. The latter has not been documented naturally but was simulated in breaking stress experiments on taenioglossan teeth (unpublished data). However, since teeth continuously enter the wearing zone they can be replaced in both scenarios.

Deformation in these structures however would be very problematic since teeth must maintain their shape while acting on ingesta. Inclusion of real material properties in our model resulted in less deformation under the load.

Each tooth region, especially pronounced in the MT, is affected differently by stress and strain: the basis and the stylus are affected more than the tooth cusps - with the exception of the small denticles that show higher values of stress and strain due to their direct interaction with the substrate. This distribution is a direct results of specific material properties: the relatively stiff and hard cusp is not affected by deformation (strain), but the flexible and soft basis and the stylus are. This pattern is not observed for the CTs and LTs showing a quite uniform distribution of both stress and strain resulting in the reduction of structural failure while scratching across the substrate surface. This system is analogous to other biological systems, such as mouthparts in Arthropods showing sclerotized and sometimes strongly mineralised cutting edges in their mouthparts enabling the crushing of food with a resistance to wear and the avoidance of structural failure [94, 96]. The function of the flexible MT basis and stylus is in providing shock absorption against mechanical impacts [123]. This behaviour, the combination of different material properties in a complex network, appears to be functionally analogous to resilin-dominated areas in Arthropods (e.g. wings or mouthparts [94, 96, 128–132], reptile skins [124, 125]), or squid beaks resulting from the regionalization of cross-linking and the degree of hydration [133–136]; the combination of a stiff and hard surface with a flexibility of underlying layers allows the structure to be less prone to failure. While foraging the MT can hence flip and rotate due to its ability to deform (this is not possible for the LTs and CTs). These findings lead to the conclusion that teeth have different functions: the CTs and LTs loosen food from the substrate whereas the MTs gather the algae from the substrate like brooms.

4.3 Mode of embedment

The central and lateral teeth have quite large attachment areas connecting the tooth basis with the membrane whereas the marginal teeth display a relatively small area (Fig. 3a). In the CT and LT forces can easily be transmitted from the tooth tip to the underlying membrane resulting in less stress and strain in the tooth structure itself, whereas the MTs have limited options transferring stress to the surrounding membrane. However, the small attachment area of the MT together with the thin and slender stylus and the material properties allows the tooth to have a stronger range of deflection.
The hardest embedding condition (membrane E=2.25 GPa) results in the lowest stress and strain mean values, but the mean stress values of the scenarios differs only little in comparison to the mean strain values. We can hence conclude that the mode of embedment has more influence on the deformation than on the stress. Stress and strain are reduced when material properties at the tooth basis and the membrane are as similar as possible. To function properly teeth have to be embedded in a membrane made of rather stiff material. The stiffness of the radular membrane itself is ensured by numerous muscles pulling it across the odontophoral cartilage while feeding.

4.4 An optimum set of model conditions and tooth functionality

Hard embedment in combination with homogenous material properties result in the smallest stress values whereas hard embedment in combination with heterogeneous material properties exhibit the lowest strain values. However, since stress values slightly differ between scenarios in contrast to strain values, we hypothesize that in radular teeth the resistance to deformation is of high importance. Besides, reduction of stress is important to avoid fracture, but snails replace the radular teeth often. Thus, the hypothetical best model condition for the teeth would be hard embedment and the presence of the material gradient.
By combining results of all FEAs we can reveal differences in functional specialisations: it seems that central and lateral teeth can transmit stresses from the cusp across the basis to the membrane. This mechanical behaviour is ensured by morphology, the large attachment area, and the interlocking system between neighbouring teeth (CT and LT support each other while feeding, which may result in more uniform stress distribution). The hardest and stiffest material is detected in the tooth cusps enabling them to loosen algae from a solid substrate with small deformation. Marginal teeth must have a different function than CTs and LTs: FEA

unravels that MTs are much more affected by stress and strain which could result in a higher risk of tooth fracture when used in the same manner.

It has been postulated that in the evolution of the taenioglossan radula (viz. the reduction in the quantity of teeth to only seven teeth/row) especially the reduction of the quantity of marginal teeth is important [25]. This is supposed to be closely related with the reduction of musculature and the shift from a sweeping to a rasping or scraping mode of feeding [137, 138], hence resulting in a more forceful way of feeding from the substrate [25]. It had been hypothesized previously, that the CTs are only used for gathering food [25, 137, 139], but our results depict that the CTs in concert with the LTs rather loosen ingesta from the substrate surface. The MTs have a different function: Steneck & Watling [25] already highlighted the possibility of marginal teeth to gather food from a greater surface area by 'inward raking' as the teeth converge to the central axis of the radula during retraction; our results comply with this hypothesis. We found that the MTs are less affected from stress and strain when the force is applied along the anterior-medial axis (Fig. 3h-j), rather supporting this 'inward raking' hypothesis. The small tooth basis as the most flexible and soft part in connection with its small attachment area with the membrane allows the flipping and rotation while retraction of the radula. During this action the comparable elongated structure of this tooth leads to a higher risk of hitting large obstacles during retraction since teeth have to cover a longer distance. The flexibility of the basis and the stylus makes the structures less prone to failure and fraction but does not allow the direct transfer of forces from the radula to the ingesta. Therefore, we postulate that the MTs rather gather food after the LTs and CTs has loosened it from the surface (see also [56]).

We here established a workflow for building substantial hypotheses on radular tooth functions. In the future we hope to address the tooth diversity of the Lake Tanganyikan Paludomidae by analysing the functionality of more teeth by FEA. Understanding how form and material properties influences the functionality allows us the allocation of adaptations and subsequently the development of possible scenarios on the evolution, including potential trophic specializations.

5. Conclusions

Here for the first time, the functionality of taenioglossan radular teeth was analysed employing Finite-Element-Analysis (FEA) resulting in values of stress and strain. We characterized the radular complex with respect to the 3D morphology, the position of each tooth, material properties, and nature of tooth attachment. To understand the relationship between tooth morphology, tooth material properties, and tooth attachment we compared 18 different FEA scenarios (representing variation in properties and fixations of the model). Our results of stress and strain mean values and distributions clearly depict different functions of teeth. We conclude that the central and lateral teeth are best structured for scratching over the substrate loosening ingesta, whereas the marginals are broom-like and best structured for collecting food particles. Further detailed biomechanical analyses of radula from other species are required to provide an integrated view of macroevolution in Mollusca as a whole.

6. Acknowledgements

We would like to acknowledge: Peter Stutz from the Mineralogical-Petrographic Institute of the University of Hamburg, Germany, and Dr. Alexander Kovalev from the Zoological Institute of the Christian-Albrechts-Universität zu Kiel, Germany, for the great support on the nanoindentation. Heinz Büscher from Basel, Switzerland, helped to great extent by collecting specimens at Lake Tanganyika. Renate Walter from the Zoological Institute of the University of Hamburg, Germany, visualized the radulae at the SEM. Thomas M. Kaiser from the CeNak Hamburg, Germany, discussed results and provided valuable suggestions to earlier versions of the manuscript. Jan-Ole Brütt from the CeNak Hamburg, Germany, provided us insight into the attachment area of the radular teeth. Lena Schwinger from the CeNak Hamburg, Germany, supported 3D printing of models. JMN acknowledges Dr. Juan Liu and the Laboratory for the Evolution and Anatomy of Fish (LEAF) of the University at Buffalo, USA, and the CERCA Programme (Generalitat de Catalunya, Spain). We are grateful for the reviews that helped to a great extent improving this paper.

7. Authors' contributions

WK wrote the manuscript, drew the figures, generated data for the model conditions and analysed the FEA data. JMN is an expert in FEA and conducted all analyses, discussed the data and wrote the manuscript. HK provided the 3D model for this analysis in the context of his bachelor thesis and discussed results. MG helped to connect the biomechanical results to molluscan biology. SG initiated, designed and planned this study, discussed the data, the manuscript, the figures; his expertise was critical for understanding the results and the functional morphology. All authors contributed to the final version of the manuscript.

8. References

[1] G. Rosenberg, A New Critical Estimate of Named Species-Level Diversity of the Recent Mollusca, Amer. Malac. Bull. 32(2) (2014) 308–322. https://doi:10.4003/006.032.0204.

[2] A.D. Chapman, Numbers of living species in Australia and the world, second ed., Toowoomba, Australia: Australian Biodiversity Information Services, 2009.

[3] S.M. Wells, Molluscs and the conservation of biodiversity, in: A.C. van Bruggen, S.M. Wells, T.C.M. Kemperman (Eds.), Biodiversity and conservation of the Mollusca, Backhuys, Oegstgeest-Leiden, Netherlands, 1995.

[4] B. Groombridge, M. Jenkins, World Atlas of Biodiversity: Earth's Living Resources in the 21st Century, University of California Press, Berkeley, California, 2002.

[5] F.W. Ponder, D.R. Lindberg, Phylogeny and Evolution of the Mollusca, University of California Press, Berkeley, 2008.

[6] M. Glaubrecht, On "Darwinian Mysteries" or molluscs as models in evolutionary biology: From local speciation to global radiation, Amer. Malac. Bull. 27 (2009) 3–23. https://doi:10.4003/006.027.0202.

[7] P. Bouchet, J.-P. Rocroi (Eds.), J. Frýda, B. Hausdorf, W. Ponder, A. Valdes, A. Warén, Classification and Nomenclator of Gastropod Families, Malacologia 47(1–2), ConchBooks, Hackenheim, Germany, 2005.

[8] M.A. Fedonkin, A. Simonetta, A.Y. Ivantsov, New data on *Kimberella*, the Vendian mollusc-like organism (White Sea region, Russia): palaeoecological and evolutionary implications, Geological Society, London, Special Publications 286(1) (2007) 157–179. https://doi:10.1144/SP286.12.

[9] P.Y. Parkhaev, Origin and the early evolution of the phylum Mollusca. Paleontol. J. 51 (2017) 663–686.

[10] A. Wanninger, T. Wollesen, The evolution of molluscs, Biol. Rev. 94 (2019) 102–115. https://doi:10.1111/brv.12439.

[11] G. Haszprunar, A. Wanninger, Molluscs, Curr. Biol. 22 (2012) 510–514. https://doi:10.1016/j.cub.2012.05.039.

[12] T. Wollesen, M. Scherholz, S.V. Rodriguez-Monje, E. Redl, C. Todt, A. Wanninger, Brain regionalization genes are coopted into shell field patterning in Mollusca, Sci. Rep. 7 (2017) 5486. https://doi:10.1038/s41598-017-05605-5.

[13] R. Guralnick, K. Smith, Historical and biomechanical analysis of integration and dissociation in molluscan feeding, with special emphasis on the true limpets (Patellogastropoda: Gastropoda), J. Morphol. 241 (1999) 175–195. https://doi:10.1002/(SICI)1097-4687(199908)241:2<175::AID-JMOR7>3.0.CO;2-0.

[14] N.W. Runham, Rate of replacement of the molluscan radula, Nature 194 (1962) 992–993. https://doi:10.1038/194992b0.

[15] N.W. Runham, A study of the replacement mechanism of the pulmonate radula, J. Cell Sci. 3 (1963) 271–277.

[16] N.W. Runham, K. Isarankura, Studies on radula replacement, Malacologia 5 (1966) 73.

[17] K. Isarankura, N.W. Runham, Studies on the replacement of the gastropod radula, Malacologia 7 (1968) 71–91.

[18] U. Mackenstedt, K. Märkel, Experimental and comparative morphology of radula renewal in pulmonates (Mollusca, Gastropoda), Zoomorphology 107 (1987) 209–239. https://doi:10.1007/BF00312262.

[19] H.A. Lowenstam, S. Weiner, Mollusca, in: H.A. Lowenstam, S. Weiner (Eds.), On Biomineralization, Oxford University Press, Oxford, 1989, 88–305.

[20] C.J. Franz, Feeding patterns of *Fissurella* species on Isla de Margarita, Venezuela: use of radulae and food passage rates, J. Molluscan Stud. 56 (1990) 25–35. https://doi:10.1093/mollus/56.1.25.

[21] D.K. Padilla, D.E. Dittman, J. Franz, R. Sladek, Radular production rates in two species of *Lacuna* Turton (Gastropoda: Littorinidae), J. Molluscan Stud. 62 (1996) 275–280. https://doi:10.1093/mollus/62.3.275.

[22] J.A. Shaw, D.J. Macey, L.R. Brooker, Radula synthesis by three species of iron mineralizing molluscs: production rate and elemental demand, J. Mar. Biol. Assoc. U.K. 88 (2008) 597–601. https://doi:10.1017/S0025315408000969.

[23] J.E. Gray, On the division of ctenobranchous gasteropodous Mollusca into larger groups and families, Ann. Mag. Nat. Hist. 11(2) (1853) 124–133. https://doi:10.1111/j.1469-7998.1853.tb07174.x.

[24] L.H. Hyman, Mollusca I. Aplacophora, Polyplacophora, Monoplacophora. Gastropoda, the Coelomate Bilateria. The Invertebrates 6, McGraw-Hill Book Company, New York, 1967.

[25] R.S. Steneck, L. Watling, Feeding capabilities and limitation of herbivorous molluscs: a functional group approach, Mar. Biol. 68 (1982) 299–319. https://doi:10.1007/BF00409596.

[26] G. Haszprunar, E. Speimann, A. Hawe, M. Heß, Interactive 3D anatomy and affinities of the Hyalogyrinidae, basal Heterobranchia (Gastropoda) with a rhipidoglossate radula, ODE 11(3) (2011). https://doi:201–236. 10.1007/s13127-011-0048-0.

[27] M. Glaubrecht, Adaptive radiation of thalassoid gastropods in Lake Tanganyika, East Africa: morphology and systematization of a paludomid species flock in an ancient lake, Zoosystematics Evol. 84 (2008) 71–122. https://doi:10.1002/zoos.200700016.

[28] F.H. Troschel, Das Gebiss der Schnecken zur Begründung einer natürlichen Classification. 1, Berlin, 1856-1863.

[29] J. Thiele, Handbuch der systematischen Weichtierkunde, Gustav Fischer, Jena, 1931–1935.

[30] N.W. Runham, The histochemistry of the radula of *Patella vulgate*, J. Cell Sci. 3 (1961) 371–380.

[31] K.M. Towe, H.A. Lowenstam, M.H. Nesson, Invertebrate ferritin: occurrence in Mollusca, Science 142 (1963) 63–64. https://doi:10.1126/science.142.3588.63.

[32] N.W. Runham, P.R. Thornton, D.A. Shaw, R.C. Wayte, The mineralization and hardness of the radular teeth of the limpet *Patella vulgata* L., Z. Zellforsch. Mikrosk. Anat. 99 (1969) 608–626. https://doi:10.1007/BF00340948.

[33] P. van der Wal, Structural and material design of mature mineralized radula teeth of *Patella vulgata* (Gastropoda), J. Ultrastruct. Mol. Struct. Res. 102 (1989) 147–161. https://doi:10.1016/0889-1605(89)90052-9.

[34] L.A. Evans, D.J. Macey, J. Webb, Distribution and composition of matrix protein in the radula teeth of the chiton *Acanthopleura hirtosa*, Mar. Biol. 109 (1991) 281–286. https://doi:10.1007/BF01319396.

[35] L.A. Evans, D.J. Macey, J. Webb, Calcium biomineralization in the radular teeth of the chiton, *Acanthopleura hirtosa*, Calcif. Tissue Int. 51 (1992) 78–82. https://doi:10.1007/BF00296222.

[36] A.P. Lee, L.R. Brooker, D.J. Macey, J. Webb, W. van Bronswijk, A new biomineral identified in the cores of teeth from the chiton *Plaxiphora albida*, J. Biol. Inorg. Chem. 8(3) (2003) 256–262. https://doi:10.1007/s00775-002-0410-y.

[37] P. van der Wal, H. Giesen, J. Videler, Radular teeth as models for the improvement of industrial cutting devices, Mater. Sci. Eng. C 7 (2000) 129–142. https://doi:10.1016/S0928-4931(99)00129-0.

[38] L. Brooker, A. Lee, D. Macey, W. Van Bronswijk, J. Webb, Multiple-front iron-mineralisation in chiton teeth (*Acanthopleura echinata*: Mollusca: Polyplacophora), Mar. Biol. 142 (2003) 447–454. https://doi:10.1007/s00227-002-0957-8.

[39] J.A. Shaw, D.J. Macey, L.R. Brooker, P.L. Clode, Tooth use and wear in three iron-biomineralizing mollusc species, Biol. Bull. 218 (2010) 132–144. https://doi:10.1086/BBLv218n2p132.

[40] J.C. Weaver, Q. Wang, A. Miserez, A. Tantuccio, R. Stromberg, K.N. Bozhilov, P. Maxwell, R. Nay, S.T. Heier, E. Di Masi, Analysis of an ultra hard magnetic biomineral in chiton radular teeth, Mater. Today 13 (2010) 42–52. https://doi:10.1016/S1369-7021(10)70016-X.

[41] L.R. Brooker, J.A. Shaw, The chiton radula: a unique model for biomineralization studies, Intech Open Access Publisher, 2012. https://doi:10.5772/31766.

[42] D. Lu, A.H. Barber, Optimized nanoscale composite behaviour in limpet teeth, J. Royal Soc. Interface 9 (2012) 1318–1324. https://doi:10.1098/rsif.2011.0688.

[43] T. Ukmar-Godec, G. Kapun, P. Zaslansky, D. Faivre, The giant keyhole limpet radular teeth: A naturally-grown harvest machine, J. Struct. Biol. 192(3) (2015) 392–402. https://doi:10.1016/j.jsb.2015.09.021.

[44] L.K. Grunenfelder, E.E. de Obaldia, Q. Wang, D. Li, B. Weden, C. Salinas, R. Wuhrer, P. Zavattieri, D. Kisailus, Biomineralization: Stress and damage mitigation from oriented nanostructures within the radular teeth of *Cryptochiton stelleri*, Adv. Funct. Mater. 24/39: 6085 (2014). https://doi:10.1002/adfm.201401091.

[45] A.H. Barber, D. Lu, N.M. Pugno, Extreme strength observed in limpet teeth, J. Royal Soc. Interface 12 (2015) 20141326. https://doi:10.1098/rsif.2014.1326.

[46] T. Ukmar-Godec, L. Bertinetti, J.W.C. Dunlop, A. Godec, M.A. Grabiger, A. Masic, H. Nguyen, I. Zlotnikov, P. Zaslansky, D. Faivre, Materials nanoarchitecturing via cation-mediated protein assembly: Making limpet teeth without mineral, Adv. Mater. 29 (2017) 1701171. https://doi: 10.1002/adma.201701171.

[47] D.H. Kesler, E.H. Jokinen, W.R. Munns Jr., Trophic preferences and feeding morphology of two pulmonate snail species from a small New England pond, USA. Can. J. Zool. 64(11) (1986) 2570–2575. https://doi:10.1139/z86-377.

[48] R. Black, A. Lymbery, A. Hill, Form and Function: size of radular teeth and inorganic content of faeces in a guild of grazing molluscs at Rottnest Island, Western Australia, J. Exp. Mar. Biol. Ecol. 121 (1988) 23–35. https://doi:10.1016/0022-0981(88)90021-4.

[49] K.R. Jensen, A review of sacoglossan diets, with comparative notes on radular and buccal anatomy, Malacological Review 13 (1980) 55–77.

[50] K.R. Jensen, Observations on feeding methods in some Florida ascoglossans, J. Molluscan Stud. 47(2) (1981) 190–199. https://doi:10.1093/oxfordjournals.mollus.a065567.

[51] K.R. Jensen, Factor affecting feeding selectivity in herbivorous Ascoglossa (Mollusca: Opisthobranchia), J. Exp. Mar. Biol. Ecol. 66(2) (1983), 135–148. https://doi:10.1016/0022-0981(83)90035-7.

[52] K.R. Jensen, Morphological adaptations and plasticity of radular teeth of the Sacoglossa (= Ascoglossa) (Mollusca: Opisthobranchia) in relation to their food plants, Biol. J. Linn. Soc. 48(2) (1993) 135–155. https://doi:10.1006/bijl.1993.1011.

[53] C.D. Trowbridge, Diet specialization limits herbivorous sea slug's capacity to switch among food species, Ecology 72(5) (1991) 1880–1888. https://doi:10.2307/1940985.

[54] W. Blinn, R.E. Truitt, A. Pickart, Feeding ecology and radular morphology of the freshwater limpet *Ferrissia fragilis*, J. N. Am. Benthol. Soc. 8(3) (1989) 237–242. https://doi: 10.2307/1467327.

[55] K. Iken, Feeding ecology of the Antarctic herbivorous gastropod *Laevilacunaria antarctica* Martens, J. Exp. Mar. Biol. Ecol. 236(1) (1999) 133–148. https://doi:10.1016/S0022-0981(98)00199-3.

[56] W. Krings, A. Kovalev, M. Glaubrecht, S.N. Gorb, Differences in the Young modulus and hardness reflect different functions of teeth within the taenioglossan radula of gastropods, Zoology 137 (2019a) 125713. https://doi:10.1016/j.zool.2019.125713.

[57] A.S.H. Breure, E. Gittenberger, The rock-scraping radula, a striking case of convergence (Mollusca), Neth. J. Zool. 32(3) (1981) 307–312. https://doi:10.1163/002829681X00347.

[58] M. Nishi, A.J. Kohn, Radular teeth of Indo-Pacific molluscivorous species of *Conus*: a comparative analysis, J. Molluscan Stud 65(4) (1999) 483–497. https://doi:10.1093/mollus/65.4.483.

[59] T.F. Duda, A.J. Kohn, S.R. Palumbi, Origins of diverse feeding ecologies within *Conus*, a genus of venomous marine gastropods, Biol. J. Linn. Soc. 73(4) (2001) 391–409. https://doi:10.1006/bijl.2001.0544.

[60] C.S. Hickman, Gastropod radulae and the assessment of form in evolutionary paleontology, Paleobiology 6 (1980) 276–294.

[61] C.S. Hickman, Ecological and phylogenetic implications of the unusual radula of *Laevinesta atlantica* (Mollusca, Gastropoda), Veliger 25 (1983) 323–325.

[62] C.S. Hickman, Implications of radular tooth-row functional-integration for archaeogastropod systematics, Malacologia 25 (1984) 143–160.

[63] T.E. Morris, C.S. Hickman, A method for artificially protruding gastropod radulae and a new model of radula function, Veliger 24 (1981) 85–89.

[64] C.S. Hickman, T.E. Morris, Gastropod feeding tracks as a source of data in analysis of the functional-morphology of radulae, Veliger 27 (1985) 357–365.

[65] D.K. Padilla, Form and function of radular teeth of herbivorous molluscs: Focus on the future, Am. Malacolog. Bull. 18 (2004) 163–168.

[66] D.K. Padilla, Structural resistance of algae to herbivores. A biomechanical approach, Mar. Biol. 90 (1985) 103–109.

[67] D.K. Padilla, Algal structural defenses: form and calcification in resistance to tropical limpets, Ecology 70 (1989) 835–842.

[68] W. Krings, T. Faust, A. Kovalev, M.T. Neiber, M. Glaubrecht, S.N. Gorb, In slow motion: radula motion pattern and forces exerted to the substrate in the land snail *Cornu aspersum* (Mollusca, Gastropoda) during feeding, R. Soc. Open Sci. 6(7) (2019b) 2054–5703. https://doi:10.1098/rsos.190222.

[69] J. Fortuny, J. Marcé-Nogué, S. de Esteban-Trivigno, L. Gil, Á. Galobart, Temnospondyli bite club: ecomorphological patterns of the most diverse group of early tetrapods, J Evol Biol. 24(9) (2011) 2040–54. https://doi:10.1111/j.1420-9101.2011.02338.x.

[70] J. Fortuny, J. Marcé-Nogué, J.-S. Steyer, S. de Esteban-Trivigno, E. Mujal, L. Gil, Comparative 3D analyses and palaeoecology of giant early amphibians (Temnospondyli: Stereospondyli), Sci Rep. 6 (2016) 30387. https://doi:10.1038/srep30387.

[71] M.R.G. Attard, W.C.H. Parr, L.A.B. Wilson, M. Archer, S.J. Hand, T.L. Rogers, S. Wroe, Virtual reconstruction and prey size preference in the mid cenozoic thylacinid, *Nimbacinus dicksoni* (Thylacinidae, Marsupialia). PLoS One 9(4) (2014) e93088. https://doi.org/10.1371/journal.pone.0093088.

[72] P. Piras, G. Sansalone, L. Teresi, M. Moscato, A. Profico, R. Eng, T.C. Cox, A. Loy, P. Colangelo, T. Kotsakis, Digging adaptation in insectivorous subterranean eutherians. The enigma of *Mesoscalops montanensis* unveiled

by geometric morphometrics and finite element analysis, J Morphol. 276(10) (2015) 1157–1171. https://doi:10.1002/jmor.20405.

[73] S. Serrano-Fochs, S. de Esteban-Trivigno, J. Marcé-Nogué, J. Fortuny, R.A. Fariña, Finite Element Analysis of the Cingulata Jaw: An Ecomorphological Approach to Armadillo's Diets, PLoS One 10(6) (2015) e0120653. https://doi:10.1371/journal.pone.0129953.

[74] A.C. Sharp, Comparative finite element analysis of the cranial performance of four herbivorous marsupials, J Morphol. 276(10) (2015) 1230–1243. https://doi:10.1002/jmor.20414.

[75] M.E.H. Jones, F. Gröning, H. Dutel, A.C. Sharp, M.J. Fagan, S.E. Evans, The biomechanical role of the chondrocranium and sutures in a lizard cranium, J R Soc Interface 14(137) (2017) 20170637. https://doi:10.1098/rsif.2017.0637.

[76] O. Panagiotopoulou, J. Iriarte-Diaz, S. Wilshin, P.C. Dechow, A.B. Taylor, H. Mehari Abraha, S.F. Aljunid, C.F. Ross, In vivo bone strain and finite element modeling of a rhesus macaque mandible during mastication, Zoology 124 (2017) 13–29. https://doi:10.1016/j.zool. 7.08.010.

[77] A.A. Farke, Frontal sinuses and head-butting in goats: a finite element analysis, J Exp Biol. 211(19) (2008) 3085–3094. https://doi:10.1242/jeb.019042.

[78] Z.J. Tseng, Cranial function in a late Miocene *Dinocrocuta gigantea* (Mammalia: Carnivora) revealed by comparative finite element analysis, Biol J Linn Soc. 96(1) (2009) 51–67. https://doi:10.1111/j.1095-8312.2008.01095.x.

[79] W.C.H. Parr, S. Wroe, U. Chamoli, H.S. Richards, M.R. McCurry, P.D. Clausen, C. McHenry, Toward integration of geometric morphometrics and computational biomechanics: New methods for 3D virtual reconstruction and quantitative analysis of Finite Element Models, J Theor Biol. Elsevier 301 (2012) 1–14. https://doi:10.1016/j.jtbi.2012.01.030.

[80] P. Aquilina, U. Chamoli, W.C.H. Parr, P.D. Clausen, S. Wroe, Finite element analysis of three patterns of internal fixation of fractures of the mandibular condyle, Br. J. Oral. Maxillofac. Surg. 51(4) (2013) 326–331. https://doi:10.1016/j.bjoms.2012.08.007.

[81] B. Figueirido, Z.J. Tseng, F.J. Serrano-Alarcon, A. Martin-Serra, J.F.F. Pastor, Three-dimensional computer simulations of feeding behaviour in red and giant pandas relate skull biomechanics with dietary niche partitioning, Biol Lett. 10(4) (2014) 20140196. https://doi:10.1098/rsbl.2014.0196.

[82] J.F. Fish, C.T. Stayton, Morphological and mechanical changes in juvenile red-eared slider turtle (*Trachemys scripta elegans*) shells during ontogeny, J Morphol. 275(4) (2014) 391–397. https://doi:10.1002/jmor.20222.

[83] J.M. Neenan, M. Ruta, J.A. Clack, E.J. Rayfield, Feeding biomechanics in *Acanthostega* and across the fish-tetrapod transition, Proc R Soc B Biol Sci. 281(1781) (2014). https://doi:10.1098/rspb.2013.2689.

[84] C.A. Brassey, J.D. Gardiner, A.C. Kitchener, Testing hypotheses for the function of the carnivoran baculum using finite-element analysis, Proc R Soc B Biol Sci. 285(1887) (2018) pii: 20181473. https://doi:10.1098/rspb.2018.1473.

[85] S. Lautenschlager, P.G. Gill, Z.-X. Luo, M.J. Fagan, E.J. Rayfield, The role of miniaturization in the evolution of the mammalian jaw and middle ear, Nature 561 (2018) 533–537. https://doi:10.1038/s41586-018-0521-4.

[86] P. Piras, L. Maiorino, L. Teresi, C. Meloro, F. Lucci, T. Kotsakis, P. Raia, Bite of the cats: Relationships between functional integration and mechanical performance as revealed by mandible geometry, Syst Biol. 62(6) (2013) 878–900. https://doi:10.1093/sysbio/syt053.

[87] L. Maiorino, A.A. Farke, T. Kotsakis, L. Teresi, P. Piras, Variation in the shape and mechanical performance of the lower jaws in ceratopsid dinosaurs (Ornithischia, Ceratopsia), J Anat. 227(5) (2015) 631–646. https://doi:10.1111/joa.12374.

[88] J. Marcé-Nogué, T.A. Püschel, T.M. Kaiser, A biomechanical approach to understand the ecomorphological relationship between primate mandibles and diet, Sci. Rep. 7 (2017) 8364. https://doi.org/10.1038/s41598-017-08161-0.

[89] J. Soons, A. Genbrugge, J. Podos, D. Adriaens, P. Aerts, J. Dirckx, A. Herrel, Is Beak Morphology in Darwin's Finches Tuned to Loading Demands?, PLoS One 10(6) (2015) e0129479. https://doi:10.1371/journal.pone.0129479.

[90] S. Miura, R. Saito, V. Parque, T. Miyashita, Design factors for determining the radula shape of *Euhadra* Peliomphala, Sci. Rep. 9(1) (2019) 749. https://doi:10.1038/s41598-018-36397-x.

[91] E.C. Aifantis, On the role of gradients in the localization of deformation and fracture, Int. J. Eng. Sci. 3 (1992) 1279–1299. https://doi:10.1016/0020-7225(92)90141-3.

[92] N. De Jager, M.D. Kler, J.M. Zel, The influence of different core material on the FEA-determined stress distribution in dental crowns, Dent. Mater. 22 (2006) 234–242. https://doi:10.1016/j.dental.2005.04.034.

[93] A. Bingbing, R. Wang, D. Arola, D. Zhang, The role of property gradients on the mechanical behavior of human enamel, J. Mech. Behav. Biomed. Mater. 9 (2012) 63–72. https://doi:10.1016/j.jmbbm.2012.01.009.

[94] J. Michels, J. Vogt, S.N. Gorb, Tools for crushing diatoms — opal teeth in copepods feature a rubber-like bearing composed of resilin, Sci. Rep. 2 (2012) 465. https://doi:10.1038/srep00465.

[95] Z. Liu, Y. Zhu, D. Jiao, Z. Weng, Z. Zhang, R.O. Ritchie, Enhanced protective role in materials with gradient structural orientations: Lessons from nature, Acta Biomater. 44 (2016) 31–40. https://doi:10.1016/j.actbio.2016.08.005.

[96] S. Büsse, S.N. Gorb, Material composition of the mouthpart cuticle in a damselfly larva (Insecta: Odonata) and its biomechanical significance, Royal Soc. Open Sci. 5 (2018) 172117. https://doi:10.1098/rsos.172117.

[97] B.D. Saltin, Y. Matsumura, A. Reid, J.F. Windmill, S.N. Gorb, J.C. Jackson, Material stiffness variation in mosquito antennae, J. R. Soc. Interface 16(154) (2019) 20190049. http://doi:10.1098/rsif.2019.0049.

[98] L.-Y. Wang, M. Jafarpour, C.-P. Lin, E. Appel, S.N. Gorb, H. Rajabi, Endocuticle sclerotisation increases the mechanical stability of cuticle, Soft Matter 15 (2019) 8272. http://doi:10.1039/c9sm01687b.

[99] E.J. Rayfield, Finite Element Analysis and Understanding the Biomechanics and Evolution of Living and Fossil Organisms, Annual Review of Earth and Planetary Sciences 35(1) (2007) 541–576. http://doi:10.1146/annurev.earth.35.031306.140104.

[100] S.P. Woodward, On some new freshwater shells from Central Africa, Proc. Zool. Soc. Lond. 27 (1859) 348-351.

[101] K.J. Boss, On the evolution of gastropods in ancient lakes, in: V. Fretter, J. Peake (Eds.), Pulmonates Systematics, Evolution and Ecology, vol. 2a, Academic Press, London, 1978, 385–428.

[102] M.R. Johnston, A.S. Cohen, Morphological divergence in endemic gastropods from Lake Tanganyika: implications for models of species flock formation, Palaios 2 (1987) 413–425. https://doi:10.2307/3514613.

[103] G.W. Coulter, Lake Tanganyika and its Life, Oxford University Press, Oxford, 1991.

[104] E. Michel, A.S. Cohen, K. West, M.R. Johnston, P.W. Kat, Large African lakes as natural laboratories for evolution: examples from the endemic gastropod fauna of Lake Tanganyika, Mitt. Internat. Verein. Limnol. 23 (1992) 85–99. https://doi:10.1080/05384680.1992.11904012.

[105] E. Michel, Why snails radiate: a review of gastropod evolution in long-lived lakes, both recent and fossil, in: K. Martens, B. Goddeeris, G.W. Coulter (Eds.), Speciation in ancient lakes, Advances in Limnology, E. Schweizerbart'sche Verlagsbuchhandlung, Stuttgart, 1994, 285–317.

[106] E. Michel, Phylogeny of a gastropod species flock: exploring speciation in Lake Tanganyika in a molecular framework, Adv. Ecol. Res. 31 (2000) 275–302. https://doi:10.1016/S0065-2504(00)31016-9.

[107] K. Martens, Speciation in ancient lakes, Trends. Ecol. Evol. 12(5) (1997) 177–182. https://doi:10.1016/S0169-5347(97)01039-2.

[108] K. West, E. Michel, The dynamics of endemic diversification; molecular phylogeny suggests an explosive origin of the thiarid gastropods of Lake Tanganyika, Adv. Ecol. Res. 31 (2000) 331–354. https://doi:10.1016/S0065-2504(00)31018-2.

[109] A.B. Wilson, M. Glaubrecht, A. Meyer, Ancient lakes as evolutionary reservoirs: evidence from the thalassoid gastropods of Lake Tanganyika, Proc. Royal Soc. Lond. B 271(1538) (2004) 529–536. https://doi:10.1098/rspb.2003.2624.

[110] E. Leloup, Exploration Hydrobiologique du Lac Tanganika (1946–1947), Bruxelles, 1953.

[111] D.S. Brown, G. Mandahl-Barth, Living molluscs of Lake Tanganyika: a revised and annotated list, J. Conchol.

32 (1987) 305–327.

[112] D. Brown, Freshwater Snails of Africa and their Medical Importance, Taylor and Francis, 1994.

[113] C.E. Kehl, J. Wu, S. Lu, D.M. Neustadter, R.F. Drushel, R.K. Smoldt, H.J. Chiel, Soft-surface grasping: radular opening in *Aplysia californica*, J. Exp. Biol. 222 (2019) jeb191254. https://doi:10.1242/jeb.191254.

[114] T.P. Neusser, M. Heβ, G. Haszprunar, M. Schrödl, Computer-based three-dimensional reconstruction of the anatomy of *Microhedyle remanei* (Marcus, 1953), an interstitial acochlidian gastropod from Bermuda, J. Morphol. 267(2) (2006) 231–247. https://doi:10.1002/jmor.10398.

[115] R.E. Golding, A.S. Jones, Micro-CT as a novel technique for 3D reconstruction of molluscan anatomy, Molluscan Res. 27(3) (2007) 123–128.

[116] W. Holznagel, A nondestructive method for cleaning gastropod radulae from frozen, alcohol-fixed, or dried material, Am. Malacol. Bull. 14(2) (1998) 181–183.

[117] D.M. Ebenstein, L.A. Pruitt, Nanoindentation of biological materials, Nano Today 1 (2006) 26–33. https://doi:10.1016/S1748-0132(06)70077-9.

[118] A.L. Smith, S. Benazzi, J.A. Ledogar, K. Tamvada, L.C.P. Smith, G.W. Weber, M.A. Spencer, P.W. Lucas, S. Michael, A. Shekeban, K. Al-Fadhalah, A.S. Almusallam, P.C. Dechow, I.R. Grosse, C.F. Ross, R.H. Madden, B.G. Richmond, B.W. Wright, Q. Wang, C. Byron, D.E. Slice, S. Wood, C. Dzialo, M.A. Berthaume, A. van Casteren, D.S. Strait, The Feeding Biomechanics and Dietary Ecology of *Paranthropus boisei*, Anat. Rec. 298(1) (2014) 145–167. https://doi:10.1002/ar.23073.

[119] D. Montroni, X. Zhang, J. Leonard, M. Kaya, C. Amemiya, G. Falini, M. Rolandi, Structural characterization of the buccal mass of *Ariolimax californicus* (Gastropoda; Stylommatophora), PLoS One 14(8) (2019) e0212249. https://doi:10.1371/journal.pone.0212249.

[120] J. Marcé-Nogué, J. Fortuny, L. Gil, M. Sánchez, Improving mesh generation in Finite Element Analysis for functional morphology approaches, Spanish J. Palaeontol. 31 (2015) 117–132.

[121] J. Marcé-Nogué, S. de Esteban-Trivigno, C. Escrig, L. Gil, Accounting for differences in element size and homogeneity when comparing Finite Element models: Armadillos as a case study, Palaeontol. Electron. 19(2) (2016) 1–22. https://doi:10.26879/609.

[122] D.G. Reid, Systematics and Evolution of *Littorina*, Ray Society, London, 1996.

[123] S.A. Herrera, L. Grunenfelder, E. Escobar, Q. Wang, C. Salinas, N. Yaraghi, J. Geiger, R. Wuhrer, P. Zavattieri, D. Kisailus, Stylus support structure and function of radular teeth in *Cryptochiton stelleri*, 20th International Conference on Composite Materials Copenhagen, 19–24th July 2015, 2015.

[124] M.-C.G. Klein, J.K. Deuschle, S.N. Gorb, Material properties of the skin of the Kenyan sand boa *Gangylophis colubrinus* (Squamata, Boidae), J. Comp. Physiol. A 196 (2010) 659–668. https://doi:10.1007/s00359-010-0556-y.

[125] M.-C. G. Klein, S.N. Gorb, Epidermis architecture and material properties of the skin of four snake species, J. R. Soc. Interface 9 (2012) 3140–3155. https://doi:10.1098/rsif.2012.0479.

[126] J.A. Shaw, L.R. Brooker, D.J. Macey, Radula tooth turnover in the chiton, *Acanthopleura hirtosa* (Blainville, 1825) (Mollusca: Polyplacophora). Molluscan Res. 22 (2002) 93–99.

[127] N.W. Runham, P.R. Thornton, Mechanical wear of the gastropod radula: a scanning electron microscope study. J. Zool. 153 (1967) 445–452.

[128] F. Haas, S.N. Gorb, R.J. Wootton, Elastic joints in dermapteran hind wings: materials and wing folding, Arthropod Struc. Dev. 29 (2000a) 137–146. https://doi:10.1016/S1467-8039(00)00025-6.

[129] F. Haas, S.N. Gorb, R. Blickhan, The function of resilin in beetlewings, Proc. R. Soc. Lond. B 267 (2000b) 1375–1381. https://doi:10.1098/rspb.2000.1153.

[130] H. Rajabi, A. Darvizeh, A. Shafiei, D. Taylor, J.H. Dirks, Numerical investigation of insect wing fracture behaviour. J. Biomech. 48 (2015) 89–94. https://doi:10.1016/j.jbiomech.2014.10.037.

[131] H. Rajabi, A. Shafiei, A. Darvizeh, S.N. Gorb, Resilin microjoints: a smart design strategy to avoid failure in dragonfly wings, Sci. Rep. 6 (2016a) 39039. https://doi:10.1038/srep39039.

[132] H. Rajabi, A. Shafiei, A. Darvizeh, J.-H. Dirks, S.N. Gorb, Effect of microstructure on the mechanical and damping behaviour of dragonfly wing veins, R. Soc. open sci. 3 (2016b) 160006. https://doi:10.1098/rsos.160006.

[133] A. Miserez, Y. Li, J.H. Waite, F. Zok, Jumbo squid beaks: inspiration for design of robust organic composites. Acta Biomater. 3 (2007) 139–149.

[134] A. Miserez, T. Schneberk, C. Sun, F.W. Zok, J.H. Waite, The transition from stiff to compliant materials in squid beaks. Science 319 (2008) 1816–1819.

[135] A. Miserez, D. Rubin, J.H. Waite, Cross-linking Chemistry of Squid Beak, J. Biol. Chem. 285 (49), (2010) 38115–38124.

[136] Y.P. Tan, S. Hoon, P.A. Guerette, W. Wei, A. Ghadban, C. Hao, A. Miserez, J.H. Waite, Infiltration of chitin by protein coacervates defines the squid beak mechanical gradient. Nat. Chem. Biol. 11 (2015) 488–495. https://doi:10.1038/nchembio.1833.

[137] V. Fretter, A. Graham, British prosobranch mollusca, their functional anatomy and ecology, Ray Society, London. 1962.

[138] A. Graham, The anatomical basis of function in the buccal mass of prosobranch and amphineuran molluscs, J. Zool. Lond. 169 (1973) 317–348.

[139] P.J.W. Jüch, G.J. Boeksehoten, Trace fossils and grazing traces produced by *Littorina* and *Lepidochitona*, Dutch Wadden Sea, Geologie en Mijnbouw 59 (1980) 33–42.

Figure 1 - adapted from [56] (a) Shells of Spekia zonata (ZMB 220.077-1); (b) schematic drawing of the radula when feeding; (c-h) taenioglossan radula of S. zonata (c-e, g : ZMB 220.144-1, f, h : ZMH 150 0 08/999-4); (c) mature worn teeth in the wearing zone; (d) CT and LT from the side; (e) immature and unworn mature CT, LT, IMT and OMT, the teeth surrounded with black lines do not show signs of wear, and hence these cusps were then modelled in Maya 3D software; (f) MT and LT manually teared out to obtain detailed information on the 3D structure; (g) IMT and OMT; (h) worn CT manually teared out to obtain detailed information on the 3D structure. Scale bars: a = 4 mm; c, e, g = 100 µm; d, h = 30 µm; f = 40 µm. CT = central tooth, FP = food particle, IMT = inner marginal tooth, IRT = immature radular teeth, LT = lateral tooth, MRT = mature radular teeth, MT = marginal tooth, O = odontophore, OMT = outer marginal tooth, RM = radular muscles, RT = radular teeth.

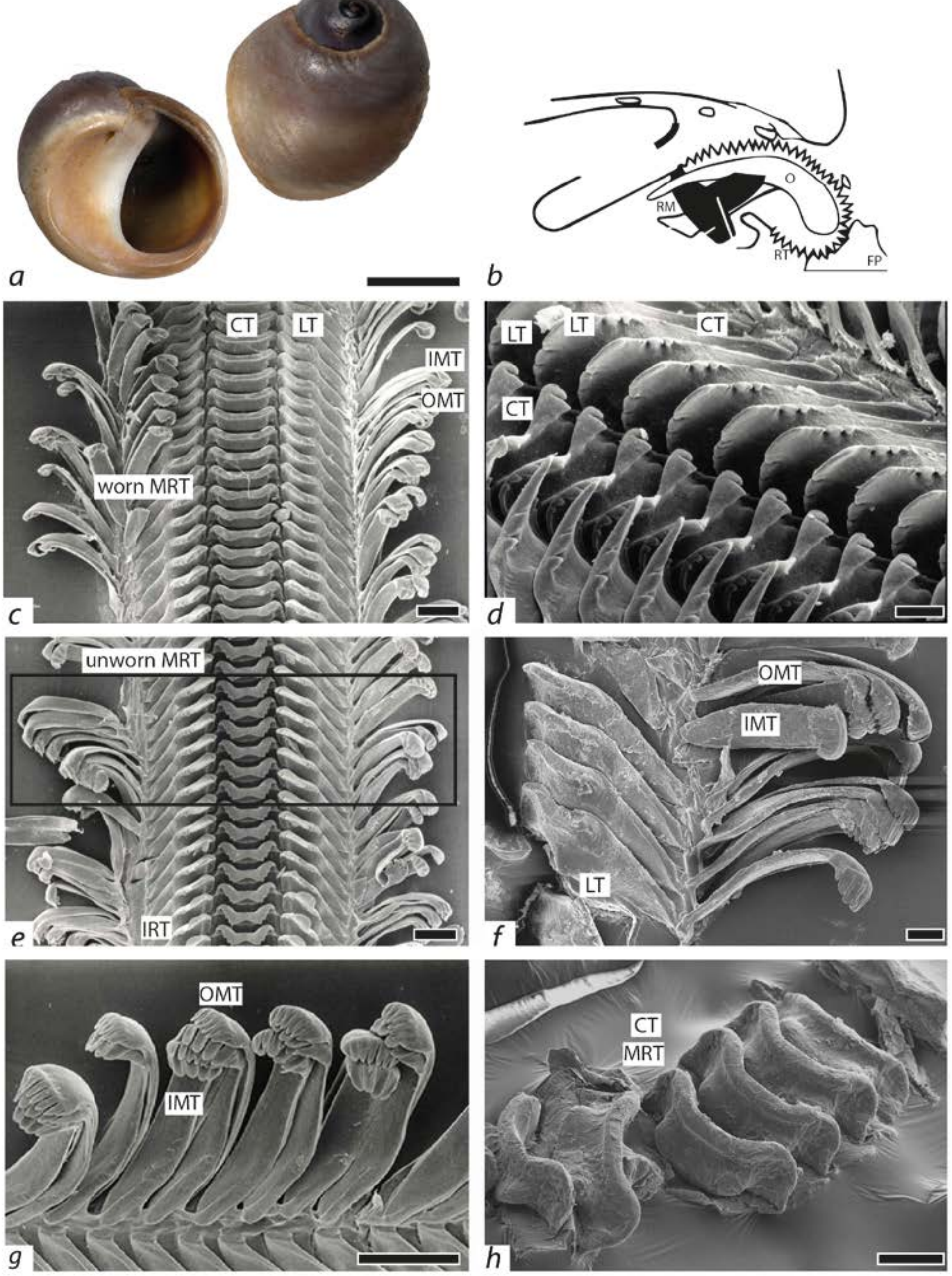

Figure 2 - 3D Modell, before creating symmetry, generated in accordance with SEM images (a) from the top view; (b) from the side; (c) from the bottom. Visualization in Meshlab 2016. CT = central tooth, IMT = inner marginal tooth, LT = lateral tooth, OMT = outer marginal tooth, TB = tooth basis, TC = tooth cusp, TS = tooth stylus.

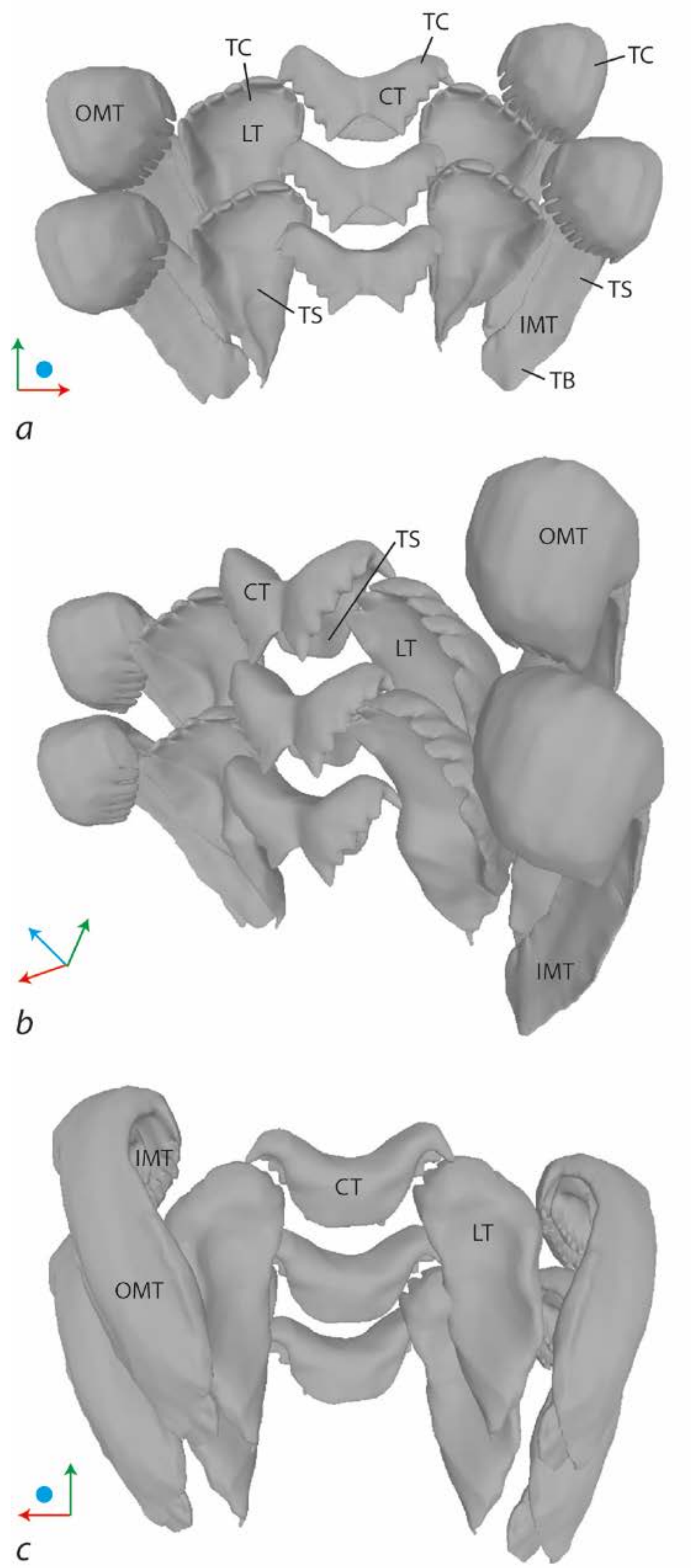

Figure 3 - Conditions for the FEA: (a) left side: cut 3D model used for FEA, right side: attachment area with the radular membrane; (b) areas with different material properties used for FEA scenarios with heterogeneous materials; area of OMT: dark blue E = 2.23 GPa, marine blue E = 3.29 GPa, blue-green E = 4.60 GPa; area of LT: dark green E = 4.95 GPa, light green E = 5.78 GPa; area of CT: yellow E = 6.67 GPa, red E = 8.09 GPa; (c-d, e-f, h-i) contact area (red) between tooth cusps and food and modelled direction of force acting on the teeth (red arrow); (e-g) first hypothetical direction of force, from anterior to posterior, for the MTs, resulting in (g) higher stress; (h-j) second hypothetical direction of force, from lateral to medial, for the MTs, resulting in (j) lower stress.

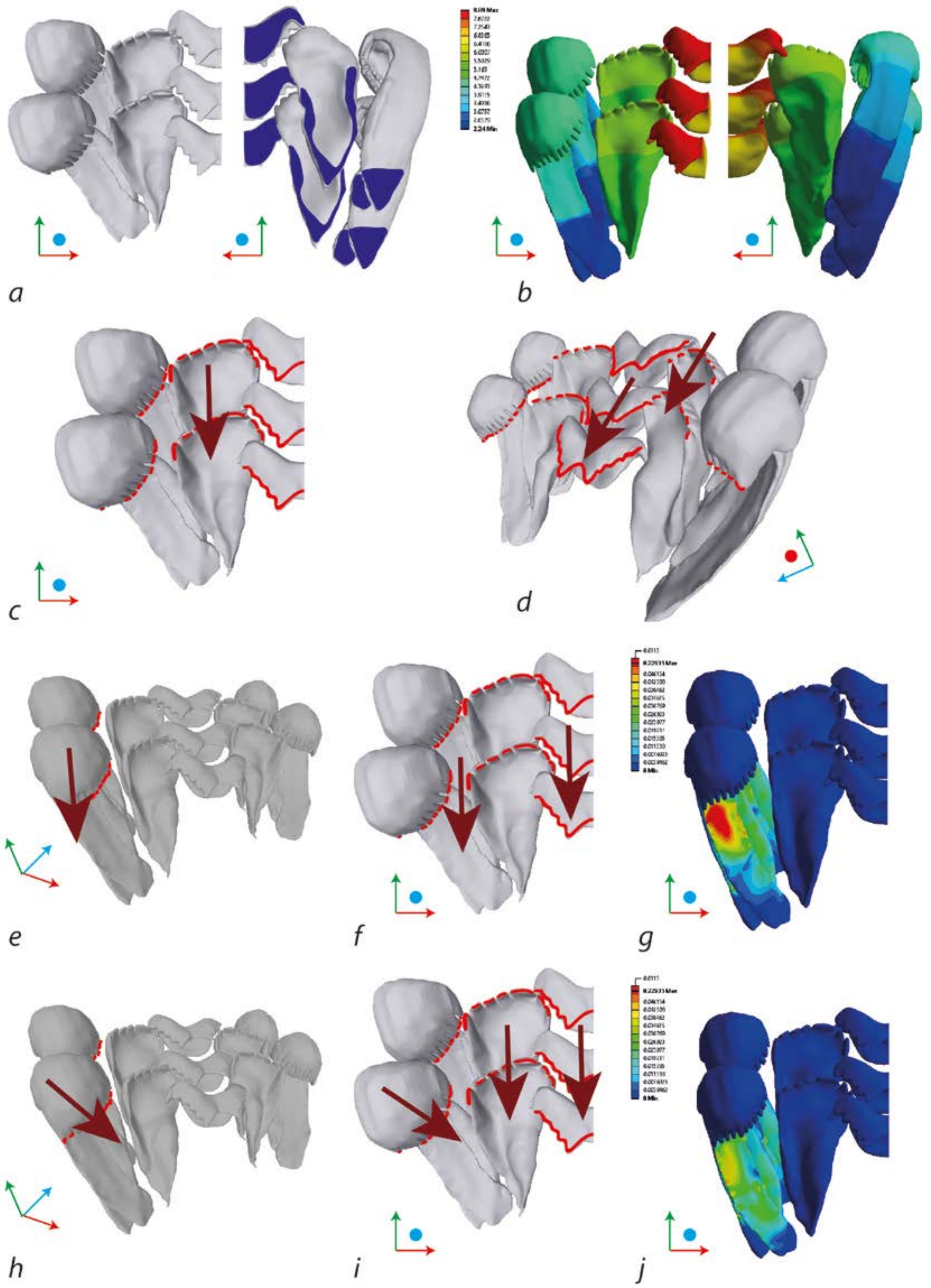

Figure 4 - Results of the FEA (stress and strain, both in MPA) for (a-f) the CT and (g-l) LT (front and back view) with soft (a-b, g-h) , medium-hard (c-d, i-j) and hard (e-f, k-l) embedding membrane. Images represent scenarios with and without material gradients, since for CT and LT there is not much difference in stress and strain values between homogenous and heterogeneous material properties (for the values of MWAM and MWM see Figs. 6 , 7 and Table 2). The scaling for Figs. 4 and 5 is identical for comparison between tooth types.

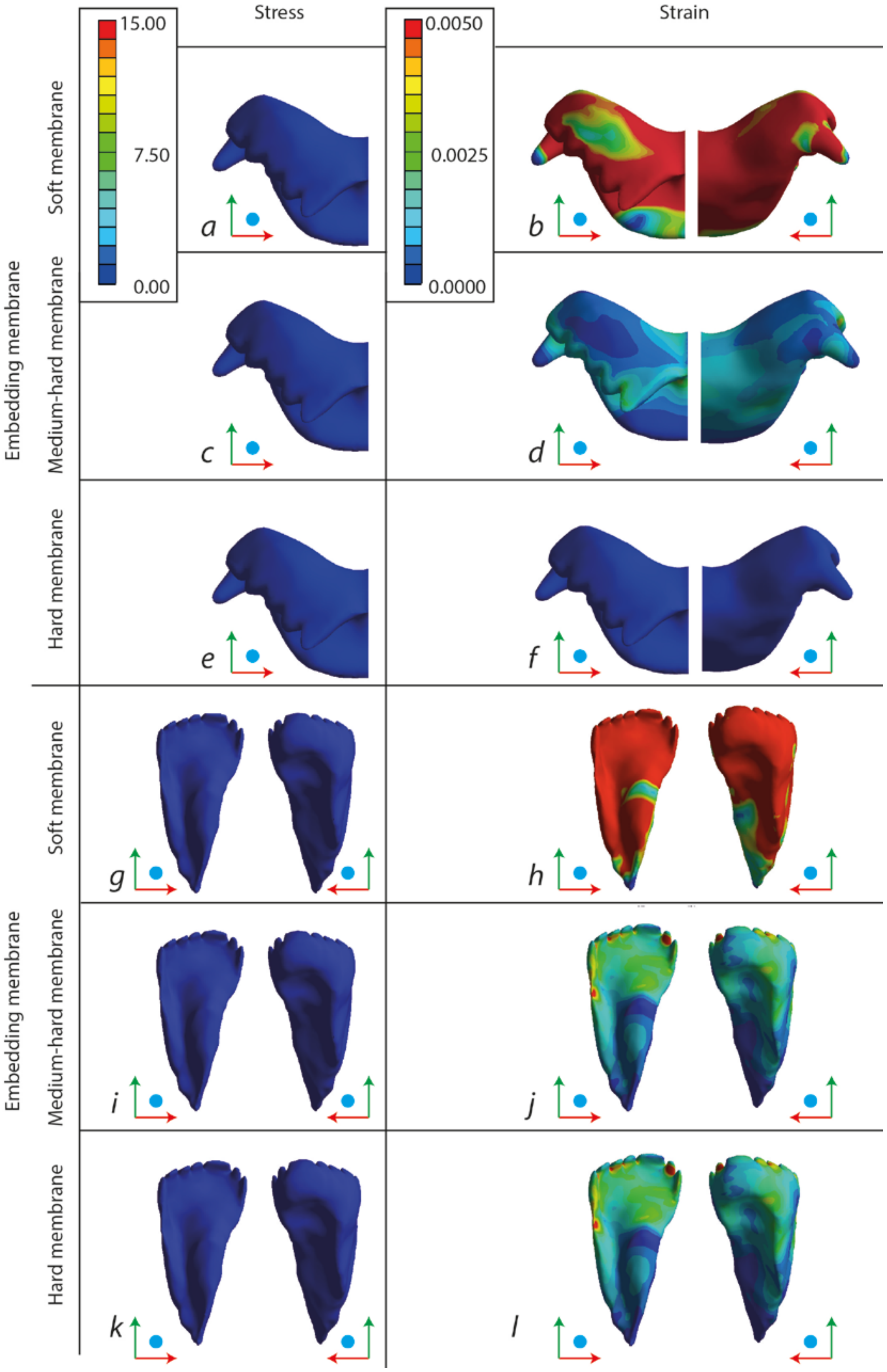

535

Figure 5 - Results of the FEA (stress and strain, both in MPA) for the OMT (front and back view) with soft (a-d) , medium-hard (e-h) and hard (i-l) embedding membrane. a, c, e, g, i, k: s cenarios without material gradient, blue circle (soft): tooth and membrane E = 0.0225 GPa, green circle (medium-hard): tooth and membrane E = 0.225 GPa, red circle (hard): tooth and membrane E = 2.25 GPa; b, d, f, h, j, l with measured material gradients (for the values of MWAM and MWM see Figs. 6 , 7 and Table 2). The scaling for Figs. 4 and 5 is identical for comparison between tooth types.

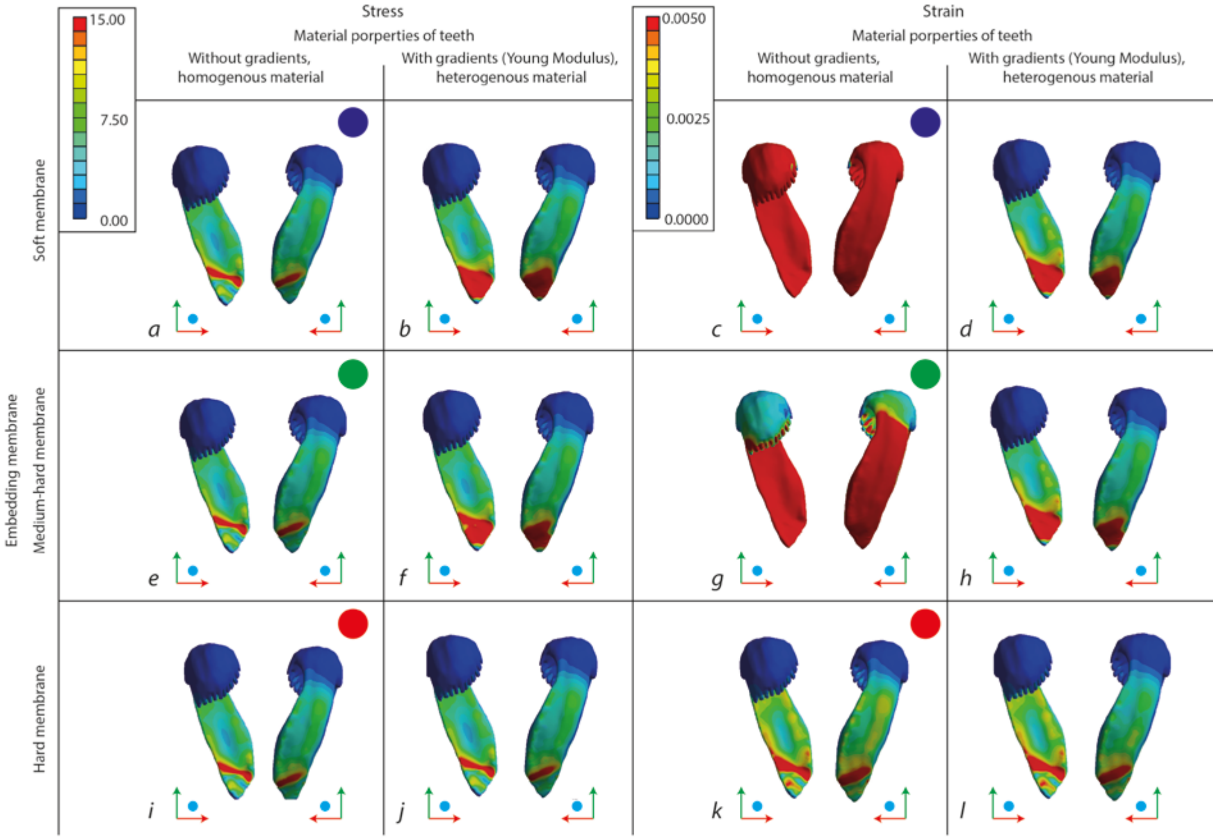

Figure 6 - Results of the FEA (values of MWAM and MWM, both in MPa) of stress and strain (lin. and log.), for the CT, LT, and OMT with different conditions of the model: embedment hard, medium-hard, soft and with or without material gradients. Blue = strain MWAM; red = strain MWM; green = stress MWAM; purple = stress MWM. For the values see Table 2

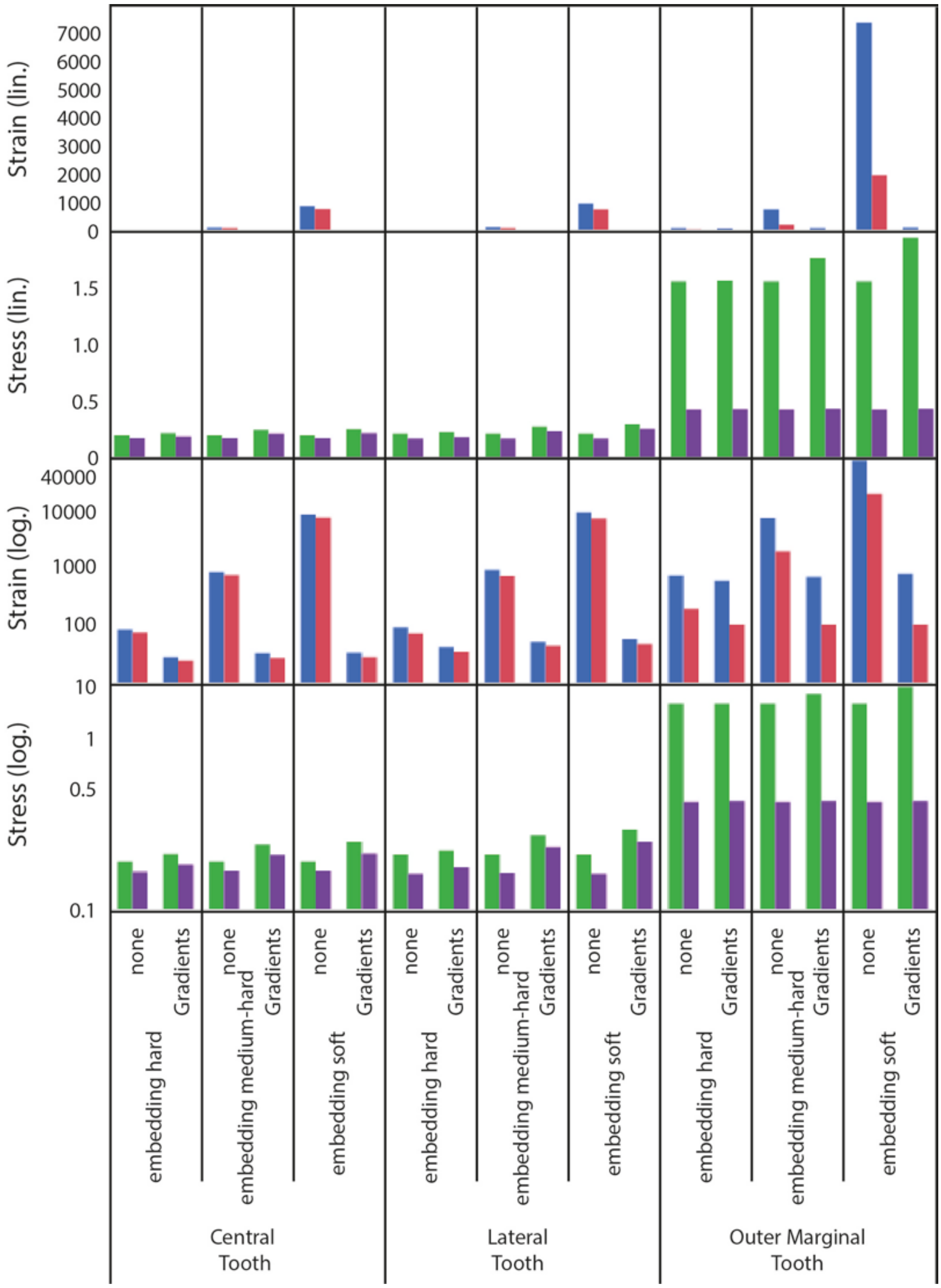

543

Figure 7 - Results of FEA, range of stress and strain values (lin. and log., both in MPa), for the CT, LT, and OMT with different conditions: embedment hard, medium-hard, soft and with or without material gradients. Blue = strain MWAM; red = strain MWM; green = stress MWAM; purple = stress MWM. For the values see Table 2

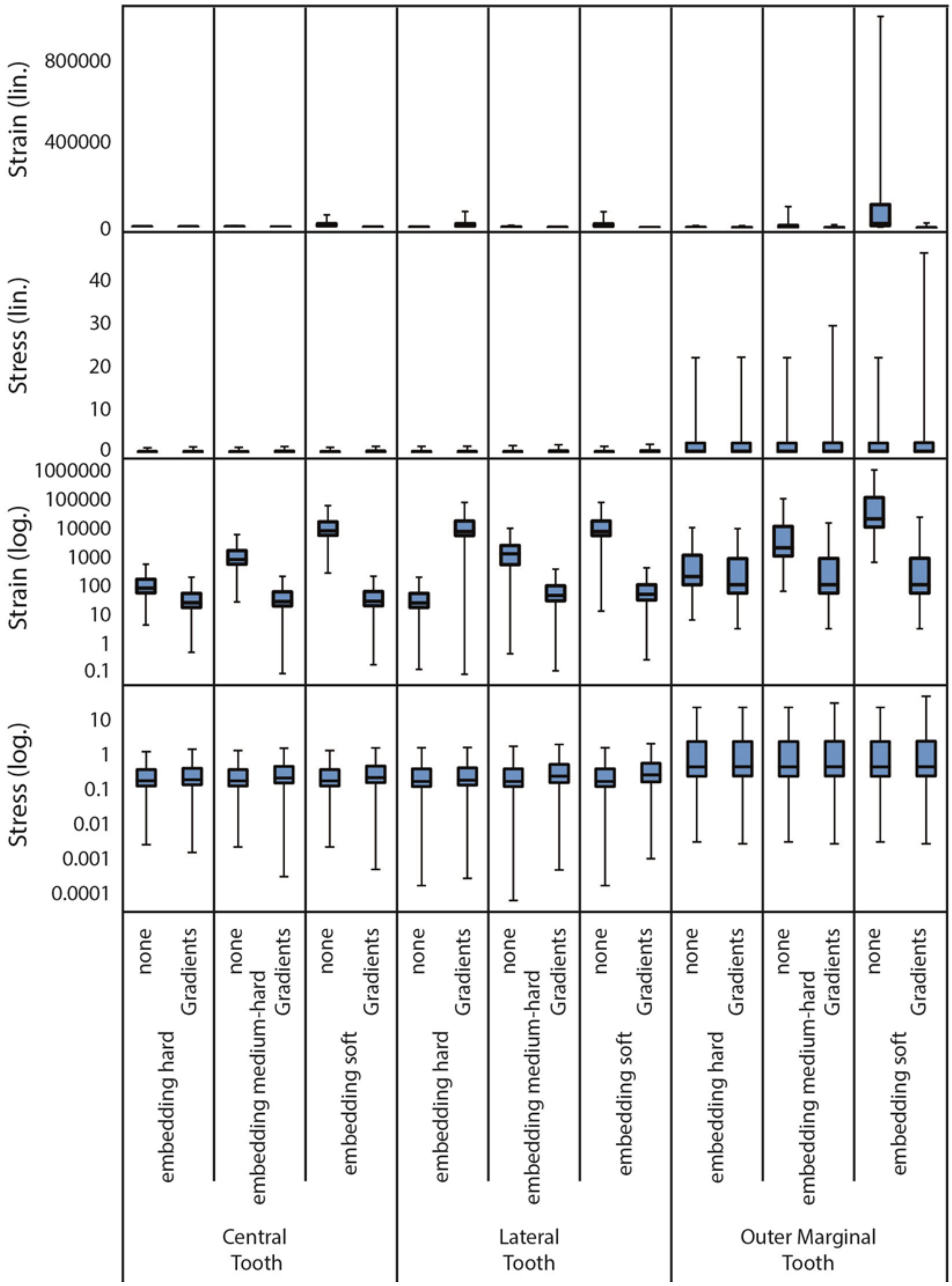

544

Figure 8 - Results of the FEA of stress and strain (b lin. and log., both in MPa) for certain defined areas (a 1-11) on the CT, LT, and OMT with different conditions of the model: embedment hard, medium-hard, soft and with or without material gradients; on the right side of the figure legend with the colour code for the different areas. For the values see Supplements Table 1